THREE-DIMENSIONAL STRUCTURE OF SOLAR WIND TURBULENCE

C. H. K. Chen[1], A. Mallet[2], A. A. Schekochihin[2], T. S. Horbury[3], R. T. Wicks[4], and S. D. Bale[1,5]

[1] Space Sciences Laboratory, University of California, Berkeley, CA 94720, USA; chen@ssl.berkeley.edu
[2] Rudolf Peierls Centre for Theoretical Physics, University of Oxford, Oxford OX1 3NP, UK
[3] The Blackett Laboratory, Imperial College London, London SW7 2AZ, UK
[4] Heliophysics Science Division, NASA Goddard Space Flight Center, Greenbelt, MD 20771, USA
[5] Physics Department, University of California, Berkeley, CA 94720, USA

ABSTRACT

We present a measurement of the scale-dependent, three-dimensional structure of the magnetic field fluctuations in inertial range solar wind turbulence with respect to a local, physically motivated coordinate system. The Alfvénic fluctuations are three-dimensionally anisotropic, with the sense of this anisotropy varying from large to small scales. At the outer scale, the magnetic field correlations are longest in the local fluctuation direction, consistent with Alfvén waves. At the proton gyroscale, they are longest along the local mean field direction and shortest in the direction perpendicular to the local mean field and the local field fluctuation. The compressive fluctuations are highly elongated along the local mean field direction, although axially symmetric perpendicular to it. Their large anisotropy may explain why they are not heavily damped in the solar wind.

Key words: magnetic fields – magnetohydrodynamics (MHD) – plasmas – solar wind – turbulence

Online-only material: color figures

1. INTRODUCTION

The solar wind is a weakly collisional plasma (e.g., Kasper et al. 2008) that is ubiquitously observed to be in a turbulent state (Tu & Marsch 1995; Goldstein et al. 1995; Horbury et al. 2005; Bruno & Carbone 2005; Petrosyan et al. 2010; Matthaeus & Velli 2011). Much progress has been made in understanding the nature of this turbulence since the first direct spacecraft observations (e.g., Siscoe et al. 1968; Coleman 1968) but many aspects are not yet fully understood. In particular, the three-dimensional (3D) structure has been poorly characterized. Here, we use a new single-spacecraft technique to measure the 3D structure of turbulence in the fast solar wind.

Turbulence is usually modeled as a local cascade of fluctuations from large to small scales, forming an inertial range. In the solar wind, most of the energy at large scales is in Alfvénic fluctuations (Belcher & Davis 1971; Bruno et al. 1985; Horbury et al. 1995; Bale et al. 2005), which have magnetic field and velocity fluctuations perpendicular to the magnetic field direction (Alfvén 1942). Early isotropic magnetohydrodynamic turbulence theories (Iroshnikov 1963; Kraichnan 1965) based on Kolmogorov scaling arguments (Kolmogorov 1941) predict that the energy spectrum of weak Alfvénic turbulence is $E(k) \sim k^{-3/2}$, where k is the wavenumber of the fluctuations. Although one-dimensional velocity power spectra in the solar wind at 1 AU display this scaling (Mangeney et al. 2001; Podesta et al. 2007; Salem et al. 2009; Chen et al. 2011a; Boldyrev et al. 2011), the magnetic field has a $k^{-5/3}$ scaling (e.g., Matthaeus & Goldstein 1982; Smith et al. 2006; Chen et al. 2011a; Boldyrev et al. 2011).

It was later realized (Montgomery & Turner 1981; Shebalin et al. 1983) that the magnetic field direction can induce anisotropy in plasma turbulence. It was then proposed (Higdon 1984; Goldreich & Sridhar 1995) that Alfvénic turbulence tends toward a state of critical balance, in which the timescale of the Alfvénic fluctuations propagating along the magnetic field is equal to the timescale of their nonlinear decay. This produces a spectrum perpendicular to the local magnetic field of $E(k_\perp) \sim k_\perp^{-5/3}$, a parallel spectrum of $E(k_\parallel) \sim k_\parallel^{-2}$ and local wavevector scaling $k_\parallel \sim k_\perp^{2/3}$. Solar wind turbulence measurements show evidence for both wavevector anisotropy of the form $k_\perp > k_\parallel$ (Crooker et al. 1982; Bieber et al. 1996; Leamon et al. 1998; Horbury et al. 2008, 2011; Podesta 2009; Wicks et al. 2010, 2011; Chen et al. 2011b) and a steeper spectral index parallel to the local magnetic field (Horbury et al. 2008, 2011; Podesta 2009; Luo & Wu 2010; Wicks et al. 2010, 2011; Chen et al. 2011b).

The critical balance theory was later extended to allow for the possibility that Alfvénic turbulence is 3D anisotropic (Boldyrev 2006). The two special orthogonal directions are the mean magnetic field $\mathbf{B}_0$ and the perpendicular magnetic field fluctuation $\delta\mathbf{B}_\perp$. The theory assumes that the magnetic field and velocity fluctuations align to within a scale-dependent angle θ_{vb}, which makes them 3D anisotropic: $l > \xi > \lambda$, where l, ξ, and λ are their correlation lengths in the mean field direction $\mathbf{B}_0$, in the $\delta\mathbf{B}_\perp$ direction, and perpendicular to both, respectively. The local spectra implied by the theory in these three directions are $E(k_l) \sim k_l^{-2}$, $E(k_\xi) \sim k_\xi^{-5/3}$, and $E(k_\lambda) \sim k_\lambda^{-3/2}$. The ξ-direction scaling follows from substituting $\xi \sim \lambda^{3/4}$ into $\delta v \sim \lambda^{1/4}$ from Boldyrev (2006), giving $\delta v \sim \xi^{1/3}$, corresponding to a local $-5/3$ spectrum.

Scale-dependent alignment has been reported in the solar wind at large scales but is difficult to measure deep in the inertial range due to instrumental limitations (Podesta et al. 2009). A recent multi-spacecraft measurement of the turbulent energy distribution in the near-Earth solar wind suggested that there was anisotropy with respect to global directions of the system, such as the global mean field, solar wind flow, or the bow shock (Narita et al. 2010b, 2010c). As far as we are aware, there has not yet been a measurement of the 3D structure of solar wind turbulence in a local, scale-dependent coordinate system (l, ξ, λ).

Although inertial range solar wind turbulence is predominantly Alfvénic, there is also a non-negligible spectrum of compressive fluctuations $\delta B_\parallel$ and δn, where n is the number density
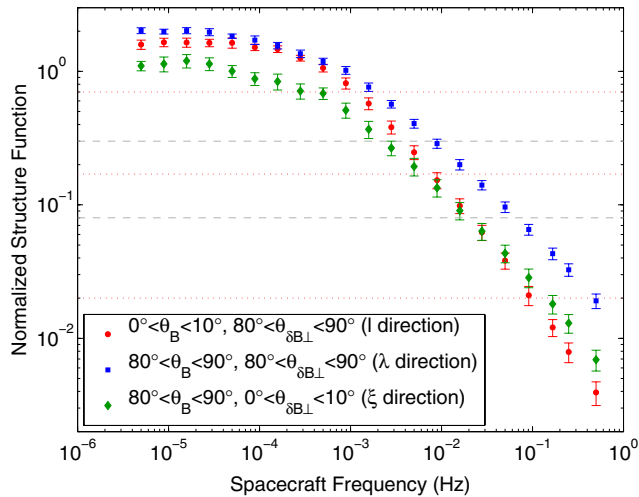
Figure 1. Normalized **B**-trace structure function in three orthogonal directions. The gray dashed lines indicate the range of values over which spectral indices were fitted. The red dotted lines correspond to the eddy shapes in Figure 4.

(A color version of this figure is available in the online journal.)
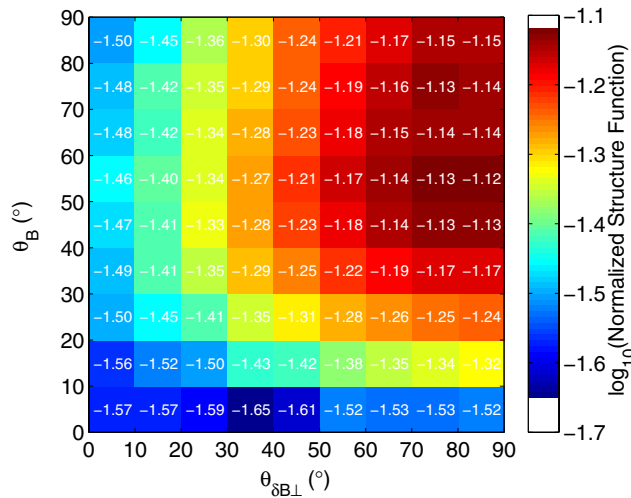
Figure 2. Normalized **B**-trace structure function at 1.5×10^{-2} Hz as a function of θ_B and $\theta_{\delta B_\perp}$.
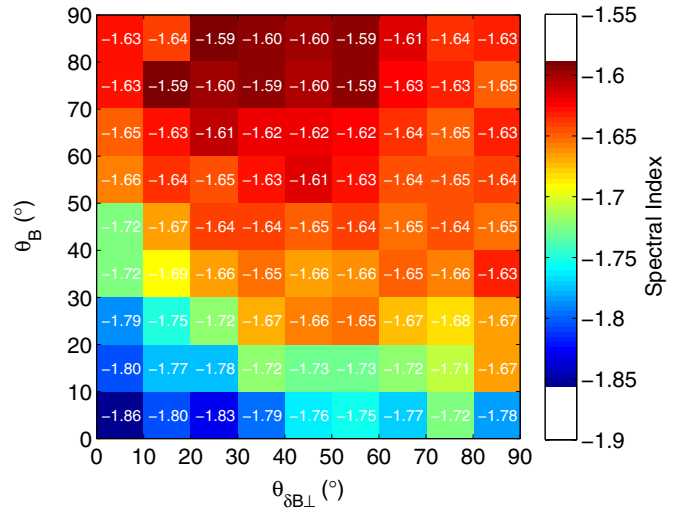
(A color version of this figure is available in the online journal.)

(e.g., Marsch & Tu 1990; Tu & Marsch 1994; Bavassano et al. 2004; Hnat et al. 2005; Kellogg & Horbury 2005; Issautier et al. 2010; Chen et al. 2011a, 2012). The nature of these fluctuations is debated (Matthaeus et al. 1991; Lithwick & Goldreich 2001; Kellogg & Horbury 2005; Schekochihin et al. 2009; Howes et al. 2012; Klein et al. 2012), in particular, the reason why they are not heavily damped. Their structure has been less comprehensively characterized than the Alfvénic turbulence, although measurements in the magnetosheath show that there is some degree of two-dimensional (2D) anisotropy (Alexandrova et al. 2008; He et al. 2011).

In this paper, we present measurements of the scale-dependent 3D structure of the Alfvénic and compressive magnetic field fluctuations with respect to a new local coordinate system and discuss the implications for our understanding of plasma turbulence.

2. METHOD

In the analysis, fast solar wind data from the *Ulysses* spacecraft (Wenzel et al. 1992) during a polar pass between 1.4 and

Figure 3. **B**-trace spectral index between normalized structure function values of 0.08 and 0.3 as a function of θ_B and $\theta_{\delta B_\perp}$.

(A color version of this figure is available in the online journal.)

2.6 AU in days 100–299 of 1995 were used. The magnetic field data from VHM (Balogh et al. 1992) were at 1 s resolution and the velocity data from SWOOPS (Bame et al. 1992) were at 4 minute resolution. The average solar wind speed was ≈ 780 km s^{-1} and the outer scale cross-helicity was moderately high, $\sigma_c \approx 0.6$ (other plasma parameters for this stream are given in Wicks et al. 2010). The data were split into 10 equal length intervals for the analysis.

For each 20 day interval, 21 logarithmically spaced spacecraft-frame frequencies at which to measure the power levels, over the range 5×10^{-6} Hz $\leqslant f_{sc} \leqslant 5 \times 10^{-1}$ Hz, were chosen. For each of these frequencies, the pairs of magnetic field measurements, $\mathbf{B}_1$ and $\mathbf{B}_2$, with the time lag $1/f_{sc}$ were selected. For each pair, the contribution to the second-order **B**-trace structure function $\sum_i (B_{1,i} - B_{2,i})^2$, where i is the component of the magnetic field, and the contribution to the second-order $|\mathbf{B}|$ structure function $(|\mathbf{B}_1| - |\mathbf{B}_2|)^2$ were calculated. Since most of the energy is in the perpendicular fluctuations (e.g., Belcher & Davis 1971), the **B**-trace spectrum is a good proxy for the Alfvénic $\delta B_\perp$ spectrum and since $|\mathbf{B}| = |\mathbf{B}_0 + \delta \mathbf{B}| \approx \sqrt{|\mathbf{B}_0|^2 + 2\mathbf{B}_0 \cdot \delta \mathbf{B}} \approx |\mathbf{B}_0| + \delta B_\parallel$, the $|\mathbf{B}|$ spectrum is a good proxy for the compressive $\delta B_\parallel$ spectrum in the inertial range, where $|\delta \mathbf{B}| < |\mathbf{B}_0|$.

It has been shown that using a local scale-dependent 2D coordinate system is important for testing theoretical predictions of spectral anisotropy (Cho & Vishniac 2000; Maron & Goldreich 2001; Horbury et al. 2008; Chen et al. 2010a, 2011b). Here, this is extended by defining a local scale-dependent 3D coordinate system. For each pair of points, the local mean field $\mathbf{B}_{local} = (\mathbf{B}_1 + \mathbf{B}_2)/2$ and the local perpendicular fluctuation direction $\mathbf{B}_{local} \times [(\mathbf{B}_1 - \mathbf{B}_2) \times \mathbf{B}_{local}]$ were calculated. The angle between $\mathbf{B}_{local}$ and the mean solar wind velocity (which is the sampling direction), θ_B, and the angle between the local perpendicular fluctuation and the component of the solar wind velocity perpendicular to $\mathbf{B}_{local}$, $\theta_{\delta B_\perp}$, were then found.

An orthogonal spherical polar coordinate system was defined, in which f_{sc} is the radial coordinate, θ_B is the polar angle, and $\theta_{\delta B_\perp}$ is the azimuthal angle. It is in this local coordinate system that the 3D anisotropy of the turbulence was measured. The structure function contributions for each f_{sc} were binned in 10° bins of θ_B and $\theta_{\delta B_\perp}$ and the mean value in each bin
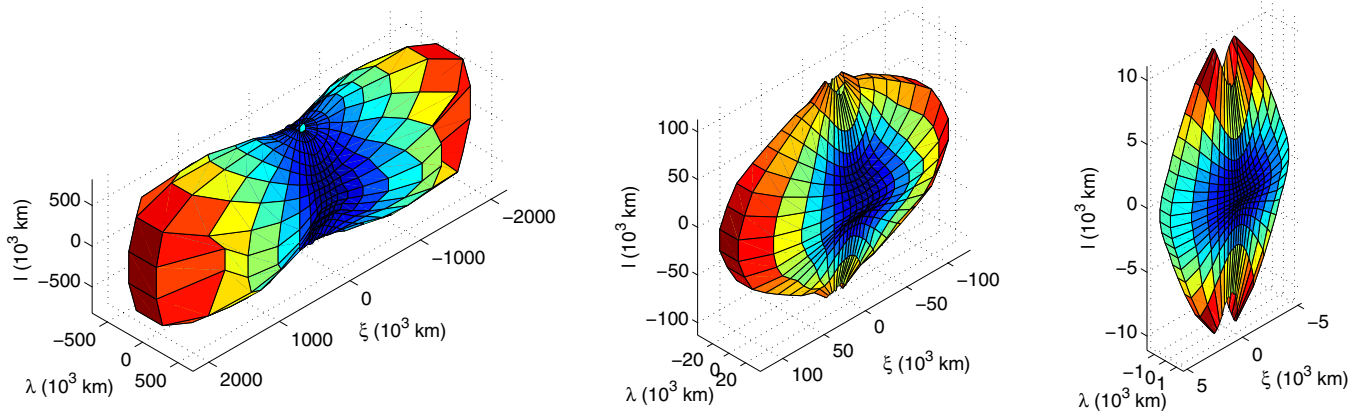
Figure 4. Surfaces of constant **B**-trace power (statistical Alfvénic eddy shapes) from large (left) to small (right) scales, in which color represents distance from the origin. The normalized power levels are 0.7, 0.17, and 0.02 as marked with red dotted lines on Figure 1. The typical proton gyroradius is ≈360 km.

(A color version of this figure is available in the online journal.)

was calculated. While the structure functions conditioned to the local field direction in this way may not be purely second order (Matthaeus et al. 2012), they are thought to be the relevant quantities in critical balance theories (Cho & Vishniac 2000; Horbury et al. 2008; Chen et al. 2011b). Any angles greater than 90° were reflected below 90° to improve accuracy for scaling measurements. Reflection in $\theta_{\delta B_\perp}$ was found to be a good approximation; while there were few points to check the validity of reflection in θ_B, the assumption seems reasonable (Podesta 2009).

Taylor's hypothesis (Taylor 1938) can be assumed for this analysis: since the speed of the solar wind moving past the spacecraft is more than 10 times the Alfvén speed in this interval (Wicks et al. 2010), temporal variations measured by the spacecraft, $1/f_{sc}$, correspond to spatial variations in the plasma v_{sw}/f_{sc}, where v_{sw} is the solar wind speed. This has been shown to be a good approximation (Narita et al. 2010a).

3. RESULTS

3.1. Alfvénic Fluctuations

Figure 1 shows the **B**-trace structure function ("power") as a function of spacecraft-frame frequency for three angle bins corresponding to the $\mathbf{B}_{local}$ direction (red circles), the $\delta\mathbf{B}_\perp$ direction (green diamonds), and the direction perpendicular to both (blue squares). Each value is the mean calculated from the 10 intervals and the error bars are 2σ, where σ is the standard error of the mean. Before averaging, the structure functions of each interval were normalized to the square of the mean field strength over the interval $\langle|\mathbf{B}|\rangle^2$ to account for the varying power levels due to the spacecraft orbit. The typical proton gyroscale corresponds to a spacecraft-frame frequency ≈0.3 Hz.

The perpendicular (blue) curve is characteristic of fast solar wind: shallow in the low-frequency $1/f_{sc}$ range (Matthaeus & Goldstein 1986) and steeper in the higher frequency inertial range. The parallel (red) curve also matches previous parallel spectrum measurements, following the perpendicular curve at low frequencies, then becoming steeper than it in the inertial range (Wicks et al. 2010). The $\delta\mathbf{B}_\perp$ (green) curve has not previously been measured and describes how the 3D anisotropy evolves in the turbulent cascade. At large scales it has a smaller value than the other structure functions, which is consistent with this range consisting of Alfvén waves (Belcher & Davis 1971), since they have wavevectors in the plane perpendicular to $\delta\mathbf{B}_\perp$.

It also remains smaller than the perpendicular structure function throughout the cascade but becomes larger than the parallel one at ≈3×10^{-2} Hz.

For each 20 day interval, a power law was fitted to the normalized structure functions between values of 0.08 and 0.3 (marked as gray dashed lines) in each angle bin. A fixed power range, rather than a fixed f_{sc} range, was used so that the scaling was measured for the same set of fluctuations (Chen et al. 2010b). For each angle bin, the fit to the structure function was evaluated at 1.5×10^{-2} Hz to give the 3D power anisotropy and the mean of the 10 intervals is shown in Figure 2. The typical standard error of the log of the mean is between 0.05 and 0.07. It can be seen that the power increases with both θ_B and $\theta_{\delta B_\perp}$, indicating 3D anisotropy, and seems to peak near $\theta_B = 60°$, $\theta_{\delta B_\perp} = 90°$.

Each fitted power-law index was converted to a spectral index by subtracting 1 (Monin & Yaglom 1975) and the 3D spectral index anisotropy is shown in Figure 3. The typical standard error of the mean is 0.01 or 0.02, although the actual uncertainty may be larger due to systematic effects, such as the finite frequency response of the structure functions. The steepening toward small θ_B (Horbury et al. 2008) can be seen but there appears to be little variation with $\theta_{\delta B_\perp}$ at large θ_B.

To visualize how the 3D anisotropy varies through the turbulent cascade, surfaces of constant power were calculated. At a selected structure function value, the corresponding frequency in each angle bin was found through linear interpolation and the scales corresponding to these frequencies were calculated using Taylor's hypothesis. The scales, together with the angles θ_B and $\theta_{\delta B_\perp}$, were converted into Cartesian coordinates (l, ξ, λ) and the surfaces of constant power (at structure function values marked by red dotted lines in Figure 1) are shown in Figure 4. They have been reflected into the other seven octants under the assumption of reflectional symmetry (see earlier). These statistical surfaces can loosely be considered as average eddy shapes (although they are not eddies in the dynamical sense). It can be seen that they change from being extended in the $\delta\mathbf{B}_\perp$ direction in the large-scale Alfvén wave range ($\xi > l, \lambda$) to being 3D anisotropic close to the proton gyroscale ($l > \xi > \lambda$).

3.2. Compressive Fluctuations

The results of a similar analysis for $|\mathbf{B}|$ are shown in Figure 5 (where the structure functions have been normalized in the same way as for the Alfvénic fluctuations in Figure 1) and
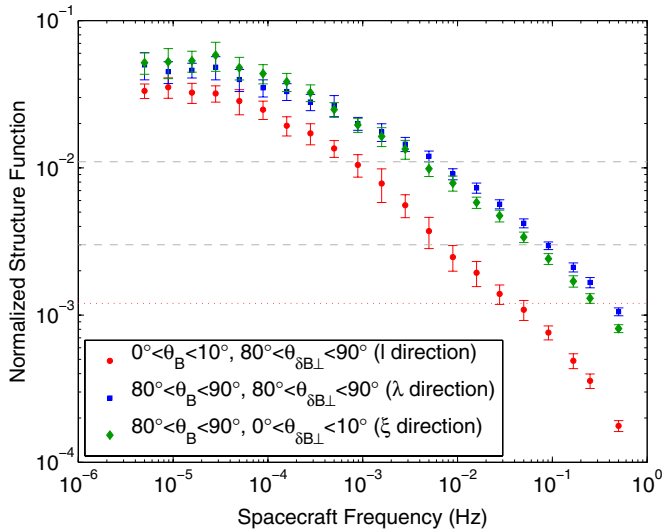
Figure 5. Normalized |**B**| structure function in three orthogonal directions. The gray dashed lines show the range of values over which spectral indices were fitted. The red dotted line corresponds to the eddy shape in Figure 6.

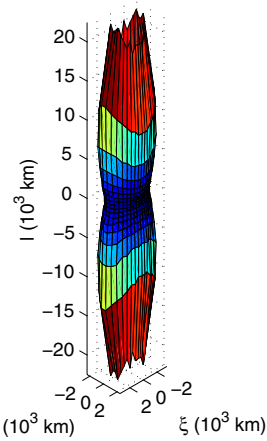(A color version of this figure is available in the online journal.)

Figure 6, which is the surface of constant normalized power of 1.2×10^{-3} (marked as a red dotted line in Figure 5). It can be seen that the structure of the compressive fluctuations is different to the Alfvénic fluctuations: there is no anisotropy in the plane perpendicular to the mean field, meaning that the compressive fluctuations do not depend on the polarization of the Alfvénic fluctuations. Also, they are more elongated along the mean field direction than the Alfvénic fluctuations: for a given perpendicular scale λ, the ratio l/λ is at least two or three times larger. Due to limited angular resolution this is a lower limit; by extrapolating the shape in Figure 6 one could imagine that they are even more extended than can currently be measured.

The spectral indices of |**B**| for normalized powers between 3×10^{-3} and 1.1×10^{-2} are between -1.58 and -1.42 in all angle bins, with a typical standard error of the mean of 0.02. This is different to the slow solar wind, where spectral indices close to $-5/3$ are observed (Chen et al. 2011a). This difference has also been noticed in the electron density spectrum (Issautier et al. 2010), although the reason is not well understood. If the compressive fluctuations are indeed very anisotropic, then we would not expect to measure the true parallel spectral index with the current angular resolution, which may explain the presence of anisotropic structures yet no significant anisotropic scaling.

4. DISCUSSION

We have shown that the Alfvénic turbulence is locally anisotropic in the plane perpendicular to the mean field. Since the direction of the anisotropy is associated with $\delta\mathbf{B}_\perp$, the question naturally arises to what extent this anisotropy is a reflection of the solenoidality of the magnetic field (Turner et al. 2011). While the magnetic field has zero divergence at each point, this does not imply that the correlation length along $\delta\mathbf{B}_\perp$ is infinite, because at any given scale we are considering finite field increments, not derivatives.

The effect of solenoidality can be derived from knowledge of the probability density function (PDF) of $\delta\mathbf{B}_\perp$. Since we are considering the conditional structure function at each scale $\langle \delta B_\perp^2 | \theta_{\delta B_\perp} \rangle$, the joint PDF $p(\delta B_\perp, \theta_{\delta B_\perp})$, or, equivalently, the PDF of the vector $\delta\mathbf{B}_\perp$ is required. As a simple illustration,

Figure 6. Surface of constant |**B**| power (statistical compressive eddy shape) at small scales. The normalized power level is 1.2×10^{-3} as marked with a red dotted line on Figure 5.

(A color version of this figure is available in the online journal.)

consider the case where this PDF is Gaussian and, therefore, fully determined by the second-order longitudinal correlation function $C_{\mathrm{LL}}(r) = \langle |\delta\mathbf{B}_\perp \cdot \mathbf{r}/r|^2 \rangle$, where $\mathbf{r}$ is the point separation in the perpendicular plane. The conditional structure function becomes

$$\left\langle \delta B_\perp^2(r) | \theta_{\delta B_\perp} \right\rangle = \frac{2 C_{\mathrm{LL}}(r) C_{\mathrm{TT}}(r)}{C_{\mathrm{LL}}(r) \sin^2 \theta_{\delta B_\perp} + C_{\mathrm{TT}}(r) \cos^2 \theta_{\delta B_\perp}}, \quad (1)$$

where the transverse correlation function is $C_{\mathrm{TT}}(r) = [r C_{\mathrm{LL}}(r)]'$ from solenoidality (Batchelor 1953). If, in the inertial range, $C_{\mathrm{LL}}(r) \propto r^\alpha$, then

$$\left\langle \delta B_\perp^2(r) | \theta_{\delta B_\perp} \right\rangle \propto \frac{r^\alpha}{1 + \alpha \cos^2 \theta_{\delta B_\perp}}. \quad (2)$$

Therefore, the ratio of the correlation scales along and across the fluctuation direction for a given structure function value is scale-independent and equal to $\xi/\lambda = (1 + \alpha)^{1/\alpha}$, which, for the measured value of $\alpha \approx 2/3$, gives an anisotropy in the perpendicular plane of ≈ 2.15. Since the measured anisotropy is larger than this (varying between 3.2 and 3.8), non-Gaussianity is required to explain the observations. Any scale-dependent alignment, e.g., the dynamical alignment of Boldyrev (2006), is likely to require non-Gaussianity and therefore be closely related to the intermittency of the turbulence.

Our results show some important differences to an earlier study, which suggested that the small-scale fluctuations are longest-correlated in one of the perpendicular directions and that the spectral index is different in all three directions (Narita et al. 2010b). Possible reasons for this include the different coordinate system used (global rather than local), the presence of foreshock effects in Narita et al. (2010b) or the different assumptions in the measurement technique.

The fact that the compressive fluctuations are very elongated is consistent with the prediction, based on gyrokinetic theory, that they are passive to the Alfvénic fluctuations, but have no parallel cascade along the exact magnetic field lines (Schekochihin et al. 2009). This may explain why there is a compressive cascade in the solar wind: the compressive fluctuations are expected to be damped at a rate proportional to their parallel wavenumber $\gamma \sim k_\parallel$ (Barnes 1966; Schekochihin et al. 2009; Klein et al. 2012) but if $k_\parallel$ is very small then they are not heavily damped

and can cascade nonlinearly. An alternative explanation is that the less anisotropic compressive fluctuations are generated but are quickly damped, leaving the highly elongated structures to be observed.

REFERENCES

Alexandrova, O., Lacombe, C., & Mangeney, A. 2008, Ann. Geophys., 26, 3585
Alfvén, H. 1942, Nature, 150, 405
Bale, S. D., Kellogg, P. J., Mozer, F. S., Horbury, T. S., & Reme, H. 2005, Phys. Rev. Lett., 94, 215002
Balogh, A., Beek, T. J., Forsyth, R. J., et al. 1992, A&AS, 92, 221
Bame, S. J., McComas, D. J., Barraclough, B. L., et al. 1992, A&AS, 92, 237
Barnes, A. 1966, Phys. Fluids, 9, 1483
Batchelor, G. K. 1953, The Theory of Homogeneous Turbulence (Cambridge: Cambridge Univ. Press)
Bavassano, B., Pietropaolo, E., & Bruno, R. 2004, Ann. Geophys., 22, 689
Belcher, J. W., & Davis, L. 1971, J. Geophys. Res., 76, 3534
Bieber, J. W., Wanner, W., & Matthaeus, W. H. 1996, J. Geophys. Res., 101, 2511
Boldyrev, S. 2006, Phys. Rev. Lett., 96, 115002
Boldyrev, S., Perez, J. C., Borovsky, J. E., & Podesta, J. J. 2011, ApJ, 741, L19
Bruno, R., Bavassano, B., & Villante, U. 1985, J. Geophys. Res., 90, 4373
Bruno, R., & Carbone, V. 2005, Living Rev. Sol. Phys., 2, 4
Chen, C. H. K., Bale, S. D., Salem, C., & Mozer, F. S. 2011a, ApJ, 737, L41
Chen, C. H. K., Horbury, T. S., Schekochihin, A. A., et al. 2010a, Phys. Rev. Lett., 104, 255002
Chen, C. H. K., Mallet, A., Yousef, T. A., Schekochihin, A. A., & Horbury, T. S. 2011b, MNRAS, 415, 3219
Chen, C. H. K., Salem, C. S., Bonnell, J. W., Mozer, F. S., & Bale, S. D. 2012, Phys. Rev. Lett., 109, 035001
Chen, C. H. K., Wicks, R. T., Horbury, T. S., & Schekochihin, A. A. 2010b, ApJ, 711, L79
Cho, J., & Vishniac, E. T. 2000, ApJ, 539, 273
Coleman, P. J. 1968, ApJ, 153, 371
Crooker, N. U., Siscoe, G. L., Russell, C. T., & Smith, E. J. 1982, J. Geophys. Res., 87, 2224
Goldreich, P., & Sridhar, S. 1995, ApJ, 438, 763
Goldstein, M. L., Roberts, D. A., & Matthaeus, W. H. 1995, ARA&A, 33, 283
He, J., Marsch, E., Tu, C., Yao, S., & Tian, H. 2011, ApJ, 731, 85
Higdon, J. C. 1984, ApJ, 285, 109
Hnat, B., Chapman, S. C., & Rowlands, G. 2005, Phys. Rev. Lett., 94, 204502
Horbury, T. S., Balogh, A., Forsyth, R. J., & Smith, E. J. 1995, Geophys. Res. Lett., 22, 3405
Horbury, T. S., Forman, M., & Oughton, S. 2008, Phys. Rev. Lett., 101, 175005
Horbury, T. S., Forman, M. A., & Oughton, S. 2005, Plasma Phys. Control. Fusion, 47, B703
Horbury, T. S., Wicks, R. T., & Chen, C. H. K. 2011, Space Sci. Rev., 293
Howes, G. G., Bale, S. D., Klein, K. G., et al. 2012, ApJ, 753, L19
Iroshnikov, P. S. 1963, AZh, 40, 742

Issautier, K., Mangeney, A., & Alexandrova, O. 2010, AIP Conf. Proc. 1216, Twelfth International Solar Wind Conference, ed. M. Maksimovic, K. Issautier, N. Meyer-Vernet, M. Moncuquet, & F. Panteuini (Melville, NY: AIP), 148
Kasper, J. C., Lazarus, A. J., & Gary, S. P. 2008, Phys. Rev. Lett., 101, 261103
Kellogg, P. J., & Horbury, T. S. 2005, Ann. Geophys., 23, 3765
Klein, K. G., Howes, G. G., TenBarge, J. M., et al. 2012, ApJ, 755, 159
Kolmogorov, A. N. 1941, Dokl. Akad. Nauk SSSR, 30, 299
Kraichnan, R. H. 1965, Phys. Fluids, 8, 1385
Leamon, R. J., Smith, C. W., Ness, N. F., Matthaeus, W. H., & Wong, H. K. 1998, J. Geophys. Res., 103, 4775
Lithwick, Y., & Goldreich, P. 2001, ApJ, 562, 279
Luo, Q. Y., & Wu, D. J. 2010, ApJ, 714, L138
Mangeney, A., Salem, C., Veltri, P. L., & Cecconi, B. 2001, in Sheffield Space Plasma Meeting: Multipoint Measurements versus Theory, ed. B. Warmbein (ESA Special Publication, Vol. 492; Noordwijk: ESA), 53
Maron, J., & Goldreich, P. 2001, ApJ, 554, 1175
Marsch, E., & Tu, C.-Y. 1990, J. Geophys. Res., 95, 11945
Matthaeus, W. H., & Goldstein, M. L. 1982, J. Geophys. Res., 87, 6011
Matthaeus, W. H., & Goldstein, M. L. 1986, Phys. Rev. Lett., 57, 495
Matthaeus, W. H., Klein, L. W., Ghosh, S., & Brown, M. R. 1991, J. Geophys. Res., 96, 5421
Matthaeus, W. H., Servidio, S., Dmitruk, P., et al. 2012, ApJ, 750, 103
Matthaeus, W. H., & Velli, M. 2011, Space Sci. Rev., 160, 145
Monin, A. S., & Yaglom, A. M. 1975, Statistical Fluid Mechanics, Vol. 2 (Cambridge, MA: MIT Press)
Montgomery, D., & Turner, L. 1981, Phys. Fluids, 24, 825
Narita, Y., Glassmeier, K.-H., & Motschmann, U. 2010a, Nonlinear Process. Geophys., 17, 383
Narita, Y., Glassmeier, K.-H., Sahraoui, F., & Goldstein, M. L. 2010b, Phys. Rev. Lett., 104, 171101
Narita, Y., Sahraoui, F., Goldstein, M. L., & Glassmeier, K.-H. 2010c, J. Geophys. Res., 115, A04101
Petrosyan, A., Balogh, A., Goldstein, M. L., et al. 2010, Space Sci. Rev., 156, 135
Podesta, J. J. 2009, ApJ, 698, 986
Podesta, J. J., Chandran, B. D. G., Bhattacharjee, A., Roberts, D. A., & Goldstein, M. L. 2009, J. Geophys. Res., 114, A01107
Podesta, J. J., Roberts, D. A., & Goldstein, M. L. 2007, ApJ, 664, 543
Salem, C., Mangeney, A., Bale, S. D., & Veltri, P. 2009, ApJ, 702, 537
Schekochihin, A. A., Cowley, S. C., Dorland, W., et al. 2009, ApJS, 182, 310
Shebalin, J. V., Matthaeus, W. H., & Montgomery, D. 1983, J. Plasma Phys., 29, 525
Siscoe, G. L., Davis, L., Jr., Coleman, P. J., Jr., Smith, E. J., & Jones, D. E. 1968, J. Geophys. Res., 73, 61
Smith, C. W., Hamilton, K., Vasquez, B. J., & Leamon, R. J. 2006, ApJ, 645, L85
Taylor, G. I. 1938, Proc. R. Soc. A, 164, 476
Tu, C.-Y., & Marsch, E. 1994, J. Geophys. Res., 99, 21481
Tu, C.-Y., & Marsch, E. 1995, Space Sci. Rev., 73, 1
Turner, A. J., Gogoberidze, G., Chapman, S. C., Hnat, B., & Müller, W.-C. 2011, Phys. Rev. Lett., 107, 095002
Wenzel, K. P., Marsden, R. G., Page, D. E., & Smith, E. J. 1992, A&AS, 92, 207
Wicks, R. T., Horbury, T. S., Chen, C. H. K., & Schekochihin, A. A. 2010, MNRAS, 407, L31
Wicks, R. T., Horbury, T. S., Chen, C. H. K., & Schekochihin, A. A. 2011, Phys. Rev. Lett., 106, 045001